AMIDE PROTON SPIN-LATTICE RELAXATION IN POLYPEPTIDES

A FIELD-DEPENDENCE STUDY OF THE PROTON AND NITROGEN DIPOLAR INTERACTIONS IN ALUMICHROME

M. LLINÁS, *Chemical Biodynamics Laboratory, University of California, Berkeley, California 94720 U.S.A., and Institute of Molecular Biology and Biophysics, ETH-Hönggerberg, 8093 Zürich, Switzerland,*

M. P. KLEIN, *Chemical Biodynamics Laboratory, University of California, Berkeley, California 94720 U.S.A.,* AND

K. WÜTHRICH, *Institute of Molecular Biology and Biophysics, ETH-Hönggerberg, 8093 Zürich, Switzerland.*

ABSTRACT The proton nuclear magnetic resonance (NMR) spin-lattice relaxation of all six amides of deferriferrichrome and of various alumichromes dissolved in hexadeutero-dimethylsulfoxide have been investigated at 100, 220, and 360 MHz. We find that, depending on the type of residue (glycyl or ornithyl), the amide proton relaxation rates are rather uniform in the metal-free cyclohexapeptide. In contrast, the ^{1}H spin-lattice relaxation times (T_1's) are distinct in the Al^{3+}-coordination derivative. Similar patterns are observed in a number of isomorphic alumichrome homologues that differ in single-site residue substitutions, indicating that the spin-lattice relaxation rate is mainly determined by dipole-dipole interactions within a rigid molecular framework rather than by the specific primary structures. Analysis of the data in terms of ^{1}H—^{1}H distances (r) calculated from X-ray coordinates yields a satisfactory linear fit between T_1^{-1} and Σr^{-6} at the three magnetic fields. Considering the very sensitive r-dependence of T_1, the agreement gives confidence, at a quantitative level, both on the fitness of the crystallographic model to represent the alumichromes' solution conformation and on the validity of assuming isotropic rotational motion for the globular metallopeptides. An extra contribution to the amide proton T_1^{-1} is proposed to mainly originate from the ^{1}H-^{14}N dipolar interaction: this was supported by comparison with measurements on an ^{15}N-enriched peptide. The nitrogen dipolar contribution to the peptide proton relaxation is discussed in the context of $\{^1H\}$—^{1}H nuclear Overhauser enhancement (NOE) studies because, especially at high fields, it can be dominant in determining the amide proton relaxation rates and hence result in a decreased effectiveness for the ^{1}H—^{1}H dipolar mechanism to cause NOE's. From the slope and intersect values of T_1^{-1} vs. Σr^{-6} linear plots, a number of independent estimates of τ_r, the rotational correlation time, were derived. These and the field-dependence of the T_1's yield a best estimate $<\tau_r> \approx 0.37$ ns, in good agreement with 0.38 ns $\lessapprox <\tau_r> \lessapprox$ 0.41 ns, previously determined from ^{13}C and ^{15}N spin-lattice relaxation data.

Dr. Llinás' present address is: Department of Chemistry, Carnegie-Mellon University, Pittsburgh, Penn. 15213.

INTRODUCTION

In spite of the sensitivity advantage afforded by proton nuclear magnetic resonance (NMR) spectroscopy, studies of the ^1H spin-lattice relaxation time (T_1) have not enjoyed the popularity of, say, ^{13}C-NMR when the conformational dynamics of polypeptides in liquid solution are investigated.

For the case of polypeptides and proteins dissolved in deuterated solvents, it is well substantiated that the proton spin-lattice relaxation processes are mostly mediated by intramolecular ^1H—^1H interactions (1–3). In particular, for the case of isotropic molecular tumbling the ^1H_i dipolar contribution to the ^1H_j relaxation rate (T_1^{-1}) is governed by Eq. 1

$$\frac{1}{T_{1_{ij}}^{i}} = \frac{3}{2}\gamma_H^4\hbar^2 I(I+1)\frac{4}{15}\frac{1}{r_{ij}^6}\left[\frac{\tau_r}{(1+\omega^2\tau_r^2)} + \frac{4\tau_r}{(1+4\omega^2\tau_r^2)}\right] \tag{1}$$

where γ_H is the proton magnetogyric ratio, $I = \frac{1}{2}$ is the proton spin, r_{ij} is the internuclear distance separating atoms H_i and H_j, τ_r is the overall molecular rotational correlation time, and $\omega = \gamma_H B$ is the angular precession frequency of the proton in the external polarizing magnetic field B (4). Eq. 1 can be rewritten

$$1/T_{1_{ij}}^{i} = Af(\omega, \tau_r)r_{ij}^{-6}, \tag{2}$$

where $f(\omega, \tau_r)$ is the expression within brackets in Eq. 1 and A contains the multiplicative constants. Eq. 2 emphasizes the fact that at a predetermined B (ω = const.), for a given spherical molecule under defined temperature and solvent conditions (τ_r = const.), the only variable left controlling the dipolar proton relaxation rate is the ^1H_i—^1H_j distance. This dependence is quite sensitive, as it appears as the sixth power of r_{ij}. The rate of spin-lattice relaxation for a single dipole pair obeys simple first-order kinetics and in the case of several interacting protons, the magnetization recovery of proton j after π-pulse inversion (5) is expressible as a sum of exponentials reflecting each single i-j dipole interaction. However, it has been observed (2, 6) that for molecules containing many H atoms

$$T_{1_j}^{-1} = Af(\omega, \tau_r)\sum_i r_{ij}^{-6}, \tag{3}$$

the $\sum_i r_{ij}^{-6}$ term effectively behaves as a geometric parameter ($\sum_j$), characterizing a magnetization recovery well fitted by a single exponential. Hence, if all the interproton distances are known, Eq. 3 indicates that a plot of $T_{1_j}^{-1}$ vs. $\sum_j$ should be linear with a slope determined by $Af(\omega, \tau_r)$. Since ω is fixed in a given experiment, a determination of $Af(\omega, \tau_r)$ affords an estimate of τ_r. Such an analysis of spin-lattice relaxation rates is novel in that usually both τ_r and $\sum_j$ are unknown, severely limiting the applicability of ^1H T_1 determinations when studying biopolymers of uncharacterized or flexible conformation(s). However, if T_1 data at different fields are available, it is possible to eliminate the distance parameter $\sum_j$ by calculating the ratio

$T_1(\omega_1)/T_1(\omega_2) = f(\omega_2, \tau_r)/f(\omega_1, \tau_r)$, containing τ_r as sole unknown (2). Unfortunately, because of instrumental limitations, T_1 field-dependence studies are often not readily accessible, which explains why T_1 determinations on ^{13}C (7, 8) or even ^{15}N (9) at fixed field are usually more informative. The one-bond C—H and N—H distances are assumed known, so that again only τ_r remains to be determined. For proteins, further ambiguities in the conformational interpretation of the proton relaxation data may arise from spin-diffusion (1, 3, 10, 11).

Ferrichrome is a microbial iron-transport ("siderophore") cyclohexapeptide that mediates the metabolic utilization of the metal in a variety of bacteria and fungi (12, 13). Alumichrome is an isomorphic (14) analogue of the naturally-occurring coordination compound, where Fe^{3+} has been substituted by diamagnetic Al^{3+}. The crystallographic structure of ferrichrome A (15) and ferrichrysin (16), two homologoues of ferrichrome that differ in two seryl-for-glycyl substitutions, are known to 0.2 Å accuracy. For this reason, and because the structure of the coordinated peptides is rigidly maintained in solution (17, 18), alumichrome (Fig. 1) has proven to be a unique model system for conformational studies of polypeptide structures by heteronuclear NMR spectroscopy (19–21). From the X-ray coordinates it is possible to position H-atoms on the C—N structural framework by using adequate orbital hybridization to account for the molecular conformation. This enables one to cal-

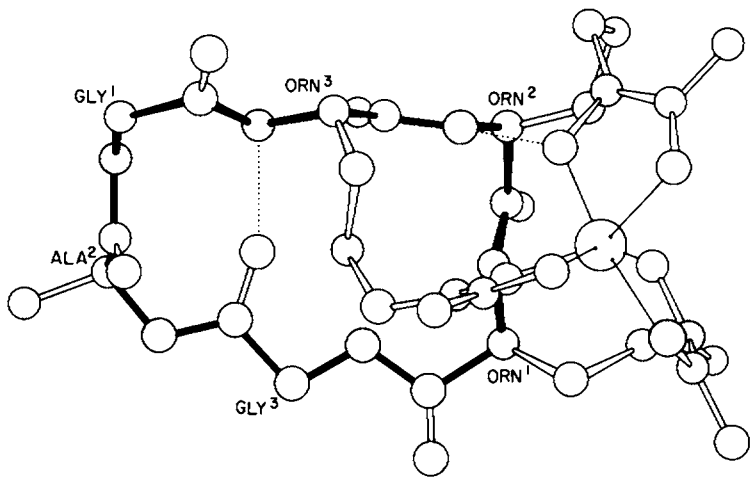

FIGURE 1 Structure of the ferrichromes (14–16). The model represents ferrichrome C. Peptide backbone bonds are denoted in heavier trace and H bonds are dotted lines (·····). For the present study Fe^{3+} was substituted by Al^{3+}. The alumichrome homologues investigated differ in the residue occupancy of sites 2 and 3 as follows:

	site 2	site 3
Alumichrome	Gly	Gly
Alumichrome C	Ala	Gly
Alumicrocin	Ser	Gly
Alumisake	Ala	Ser
Alumichrysin	Ser	Ser

culate the $\sum_j$ parameters for protons that exhibit well-resolved NMR signals so that the experiment described above can be performed to estimate τ_r from proton T_1 data.

In this communication we report on a series of peptide proton T_1 studies at 100, 220, and 360 MHz (B = 2.349 T, 5.168 T, and 8.456 T, respectively). The investigation focused on the amide proton resonances which, because of their chemical shift sensitivity to H-bonding, are usually well resolved and have thus become most valuable conformational probes in structural studies by NMR spectroscopy (22–24).

METHODS

The source, preparation, and purification of the alumichrome peptides have been reported elsewhere (17–21). In particular, the deferriferrichrome, alumichrome, and [^{15}N]alumichrome samples were the same as those used in two previous NMR spin-lattice relaxation studies (8, 9). All peptide samples were dissolved to 0.15 M in hexadeutero-dimethylsulfoxide (d_6-DMSO) after repeated extractions with 8-hydroxyquinoline (8) to remove contaminating paramagnetic metal ions, mainly Fe^{3+}. Consistent with observations of other investigators (25, 26), degassing the sample to eliminate O_2 had no detectable effect on the measured proton relaxation rates.

The T_1's were determined by the $(180\text{-}\tau\text{-}90\text{-}5T_1)_n$ sequence of Vold et al. (5). We have not observed any significant deviation from single exponential behavior in the magnetization recovery after a π-pulse which indicates that Eq. 3 is a valid approximation for this study. The measurements at 100 and 360 MHz were performed at the ETH-Hönggerberg with a Varian XL-100 (Varian Associates, Palo Alto, Calif.) and a Bruker HXS-360 spectrometer (Spectrospin A.G., Fällanden, Zürich), respectively. The spectra at 220 MHz were recorded with a Varian HR 220 instrument modified for Fourier performance (University of California at Berkeley). Temperatures were determined to ±2°C with a sealed tube of ethylene glycol standard and the temperature calibration charts provided by the instrument manufacturers. All T_1's reported here are accurate to more than 5% in the linear least squares standard deviations of the semilogarithmic magnetization recovery plots (correlation coefficients > 0.99).

RESULTS

After π-pulse inversion, the metal-free peptide, deferriferrichrome, exhibits a relatively uniform recovery of the amide ^{1}H magnetization. Under the specified experimental conditions, Fig. 2 shows that the amide resonances change the magnetization sign at $\tau \sim 160$ ms, the ornithyl doublets appearing to relax somewhat faster ($< T_1 >$ = 238 ms) than the glycyl triplets ($< T_1 >$ = 300 ms). Consistent with previous ^{13}C (8, 27) and ^{15}N (9) NMR relaxation studies, this indicates that the triglycyl segment is somewhat more flexible than the triornithyl sequence. Furthermore, the similar relaxation rates for each homotripeptide suggest identical dipole-dipole distances for residues within each segment. This would result from a relaxed conformation that accommodates to minimize interatomic repulsive forces, thus achieving a distance parameter value about equal for all residues of the same kind. The pattern shown by Fig. 2 is reminiscent of the trend exhibited by the gramicidin S NH's (23, 28), indicative of an overall lack of backbone conformational rigidity for that cyclodecapeptide as well. The situation is drastically different for alumichrome.

After metal complexation, the amides become distinct in terms of chemical shifts

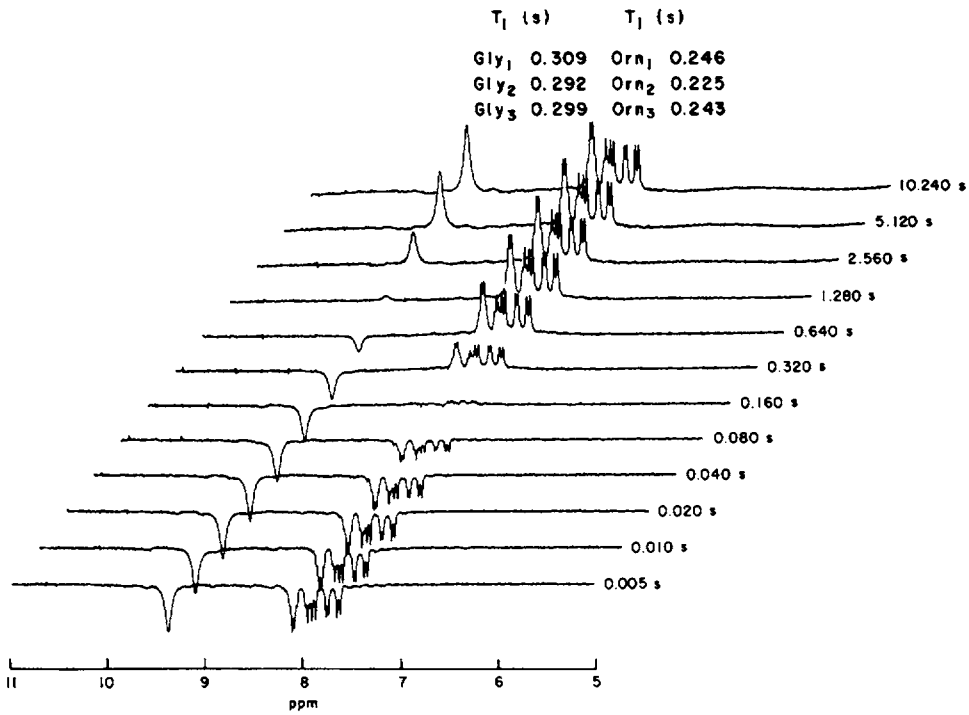

FIGURE 2 Sequence of partially relaxed spectra of deferriferrichrome at 220 MHz (0.15 M in d_6-DMSO, $t \approx 81°C$). The six amide signals appear between ca. 7.5 and 8.3 ppm. Gly NH resonances triplets appear at lower field from the ornithyl doublet positions. The broad resonance at ~9.3 ppm arises from the free hydroxamic acid NO*H* group. Measured T_1 values are indicated. The spectrum has been described elsewhere (14 and references therein).

(14). Concomitantly, Fig. 3 shows that the T_1 values spread over a wider range. As revealed by the τ = 160 ms spectrum, the Orn^1 and Orn^2 resonances are above the base line when the other four amides are still negative. Thus, while the Gly^1, Gly^2, and Gly^3 NH's relax with T_1 = 304, 361, and 401 ms, respectively, the ornithyl amides cover a still wider range, with T_1 = 156, 221, and 392 ms for Orn^2, Orn^1, and Orn^3, respectively. That is, once the tertiary structure becomes "frozen" in the metallopeptide, the six amides relax at rates that no longer reflect the particular residue type but rather the distance parameter $\sum_j$ characterizing the dipolar interactions in the rigid spatial structure.

We have studied a variety of deferriferrichrome and alumichrome analogues which differ in the residue occupancy of sites 2 and 3 (alanyl or seryl residues substituting for Gly^2 and Gly^3; Fig. 1). A consistent pattern has been observed: while the metal-free, flexible cyclohexapeptides show uniform relaxation rates, the Al^{3+}-coordinated derivatives exhibit the type of site differentiation exemplified by the spectrum in Fig. 3, and this is independent of temperature (observed at t = 22°, 45°, 66°, 81°, and 97°C). Expectedly, because of a drop in solvent viscosity, all T_1's become longer

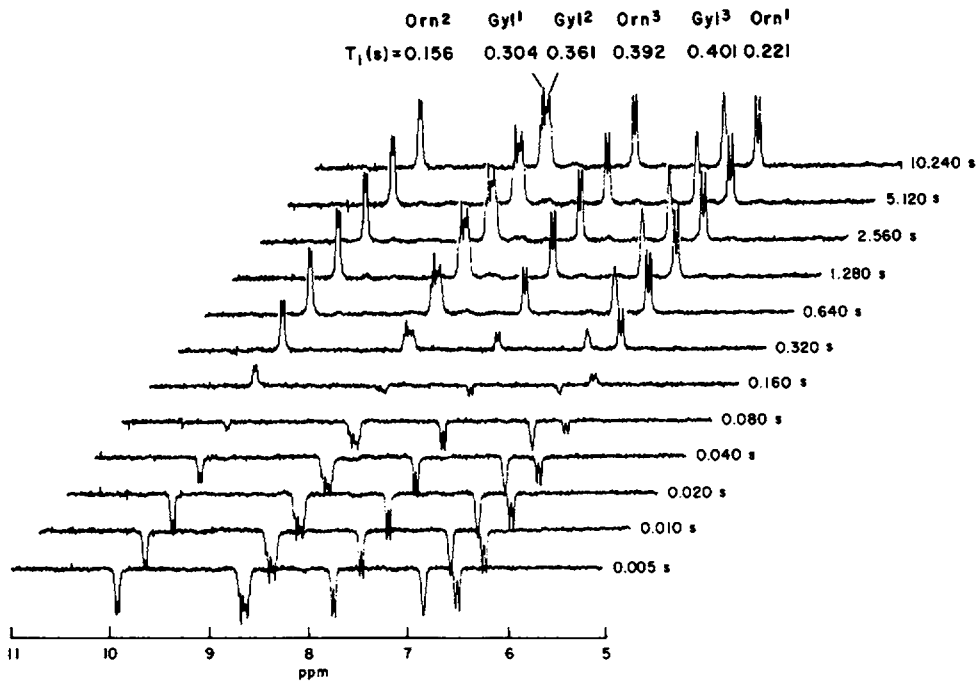

FIGURE 3 Sequence of partially relaxed amide spectra of alumichrome at 220 MHz (0.15 M in d_6-DMSO, $t \approx 81°C$). Resonance assignments and measured T_1 values are indicated. The spectrum has been described elsewhere (14, 18).

at higher temperatures. In what follows, we focus the discussion on data measured at 44°C, since earlier ^{13}C and ^{15}N experiments were performed at that temperature (8, 9). Table I lists T_1's at 220 MHz for all the alumichrome homologues we have studied and shows that the overall amide T_1 pattern remains basically unaffected to the extent that even sites 2 and 3 are essentially insensitive as to whether they are occupied by Ala, Gly, or Ser residues.

TABLE I
AMIDE PROTON SPIN-LATTICE RELAXATION TIMES OF ALUMICHROME HOMOLOGUES

	Gly^1	Site 2	Site 3	Orn^1	Orn^2	Orn^3
Alumichrome	223	264 (G)	275 (G)	166	134	278
Alumichrome C	203	269 (A)	258 (G)	164	132	286
Alumicrocin	199	245 (S)	282 (G)	179	135	259
Alumisake	236	258 (A)	244 (S)	171	123	279
Alumichrysin	210	239 (S)	230 (S)	162	145	281
[^{15}N]alumichrome	271	293 (G)	334 (G)	253	162	369

T_1 values (milliseconds) determined at 220 MHz, 0.15 M solutions in d_6-DMSO at 44°C. Residue occupancy of sites 2 and 3 are indicated in parenthesis: A, alanine; G, glycine; S, serine.

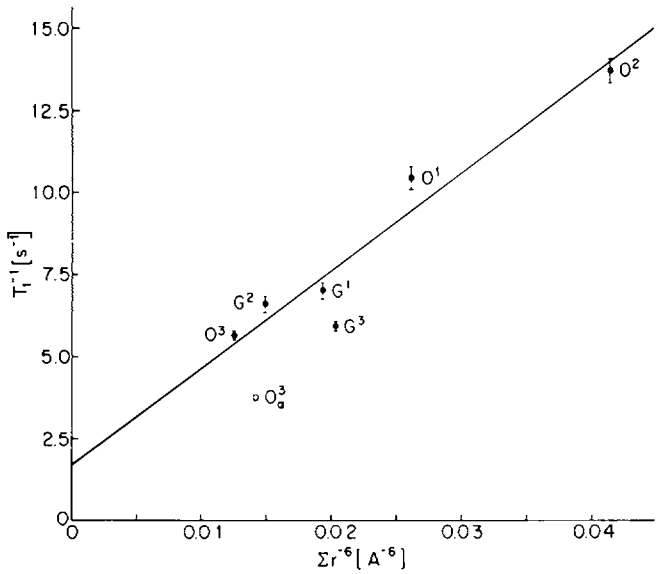

FIGURE 4 Linear least squares plot of T_1^{-1} versus distance parameter Σ for the alumichrome amides (100 MHz, 0.15 M solution in d_6-DMSO, t = 44°C). NH data are represented by full circles (●) while the Orn^{3}C$_\alpha$H measurement, not considered in the linear fit, is denoted by an open circle (○). Experimental uncertainties are included. The data are listed in Tables II and III.

In addition to those at 220 MHz, the amide proton spin-lattice relaxation rates have been measured at 100 and 360 MHz. Fig. 4 shows the NH T_1^{-1}'s at 100 MHz (full circles) plotted against the geometrical dipolar parameter $\sum_j$ calculated from the C,N crystallographic coordinates of ferrichrome A (15) after positioning H atoms with 1.04 and 1.09 Å for the N—H and C—H bond distances, respectively (Table II). By least-squares fitting a straight line to the six amide data points, a reasonable match (r = 0.95) between the NMR T_1^{-1} values and the crystallographic Σr^{-6} distance

TABLE II
ALUMICHROME AMIDE DISTANCE PARAMETERS AND FIELD DEPENDENCE OF THE RELAXATION RATES

	Σr_{HH}^{-6}	T_1^{-1}		
		100 MHz	220 MHz	360 MHz
	$Å^{-6} \times 10^2$		s^{-1}	
Gly^1	1.93	7.02	4.48	2.94
Gly^2	1.49	6.62	3.78	2.58
Gly^3	2.03	5.93	3.64	2.42
Orn^1	2.62	10.47	6.02	3.60
Orn^2	4.14	13.70	7.46	4.46
Orn^3	1.25	5.66	3.60	2.33

parameter can be obtained: $T_{ij}^{-1} = 298.6 \sum_j + 1.7\,s^{-1}$. The slope measures $A \cdot f(\omega, \tau_r)$ in Eq. 3, which, with $\nu = \omega/2\pi = 100$ MHz, directly yields $\tau_r = 4.2 \times 10^{-10}$ s. The intercept at the origin indicates other relaxation processes, extra to $^1H—^1H$ dipolar interactions, not included in Eqs. 1–3.

Contrary to common belief, a scalar mechanism of the second kind (29) arising from modulation of the $^{14}N—^1H$ spin-spin coupling by quadrupolar relaxation of the nitrogen nucleus, can be immediately excluded as a contributor of any significance to the NH proton magnetization recovery. Assuming $^1J_{HN} \sim 90$ Hz (19), it can be readily estimated (29) that such a process would, at most, contribute $T_1^{-1} \sim 10^{-5}\,s^{-1}$, negligible when compared with the measured rates.

In a previous communication (9) we have reported on the nitrogen relaxation of [^{15}N] alumichrome at 10.1 MHz and have shown that it is dominantly caused by dipole-dipole interaction with the amide proton. It is hence predictable that the amide $^{14}N—^1H$ dipolar interaction also ought to be sensed by the proton magnetization. We claim that the extra contribution to the amide proton relaxation determined from the ordinate intercept in Fig. 5 is to a great extent due to this heteronuclear dipolar mechanism. This contention is given support by the rate of the Orn^3 $^1H^\alpha$ magnetization recovery. This aliphatic resonance appears well-resolved, next, at higher fields, to the amide region. Fig. 5 shows a partially relaxed spectrum at 360 MHz ($\tau = 240$ ms) spanning the 4.5 ppm $< \delta <$ 10.5 ppm spectral region. As illustrated, the amide protons lead the Orn^3 $^1H^\alpha$ in the longitudinal magnetization recovery. In Fig. 4, the Orn^3 $^1H^\alpha$ T_1^{-1} has been included (open circle); as indicated, this aliphatic proton exhibits $\Sigma = 1.33 \times 10^{-2}$ Å^{-6}, a distance parameter value comparable to those of the Orn^3 or Gly^3 amide proton (Table II). However, its location on the graph (Fig. 4) is significantly *below* the position determined by the NH line, the shift being 1.8 s^{-1}, i.e., close to the ordinate intercept value of 1.7 s^{-1}.

The nitrogen dipolar relaxation of the proton magnetization is governed by Eq. 4 (4).

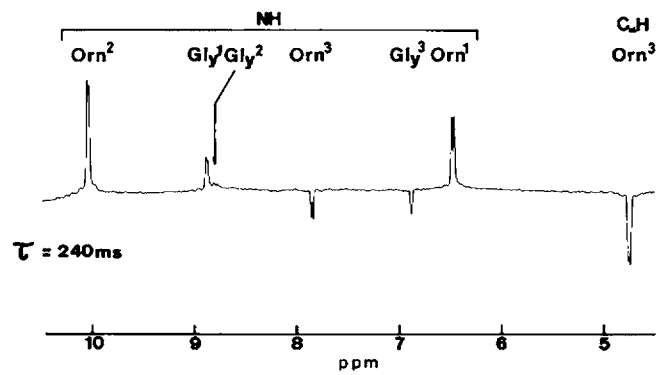

FIGURE 5 Partially relaxed spectrum of the low field resonance region of alumichrome at 360 MHz ($\tau = 240$ ms, 0.15 M in d_6-DMSO, $t = 44°C$).

$$\frac{1}{T_1}_{NH} = \frac{4}{30}\hbar^2\gamma_H^2\gamma_N^2\langle r_N^{-6}\rangle I_N(I_N + 1)$$

$$\cdot\left[\frac{\tau_r}{1 + (\omega_H - \omega_N)^2\tau_r^2} + \frac{3\tau_r}{1 + \omega_H^2\tau_r^2} + \frac{6\tau_r}{1 + (\omega_H + \omega_N)^2\tau_r^2}\right] \quad (4)$$

where γ_N is the nitrogen nuclear magnetogyric ratio, I_N the nitrogen nuclear spin, ω_N, the nitrogen NMR angular frequency, and r_N is the N—H internuclear distance (= 1.04 Å). If the $^{14}N—^1H$ dipolar interaction is the only relaxation mechanism besides $^1H—^1H$ dipolar interactions, the intercept value in Fig. 4 yields, on the basis of Eq. 4, an independent estimate of the isotropic rotational correlation time, $\tau_r = 2.8 \times 10^{-10}$ s, close to that derived from the linear fit slope, $\tau_r = 4.2 \times 10^{-10}$ s.

Independent evidence for the role of nitrogen in determining the amide relaxation is afforded by comparing ^1H longitudinal relaxation rates determined from ^{14}N (natural abundance) and 99.2% ^{15}N-enriched peptides. Inserting the proper parameter values characterizing the two nitrogen isotopes [I = 1 (^{14}N), $\frac{1}{2}$ (^{15}N); γ = 0.1934 (^{14}N), −0.2712 (^{15}N) rad · s^{-1} · T^{-1}; ν = 15.89 (^{14}N), 22.29 (^{15}N) MHz for 200 MHz (^1H)] into Eq. 4, one can predict that the nitrogen dipolar contribution to the proton T_1^{-1} should decrease by a factor of 0.73 on going from the ^{14}N to the ^{15}N peptide. In other words, the ^{14}N and ^{15}N peptides ought to yield similar dependencies when T_{ij}^{-1} is plotted vs. $\sum_j$ but with the ^{15}N peptide line displaced *below* that of the

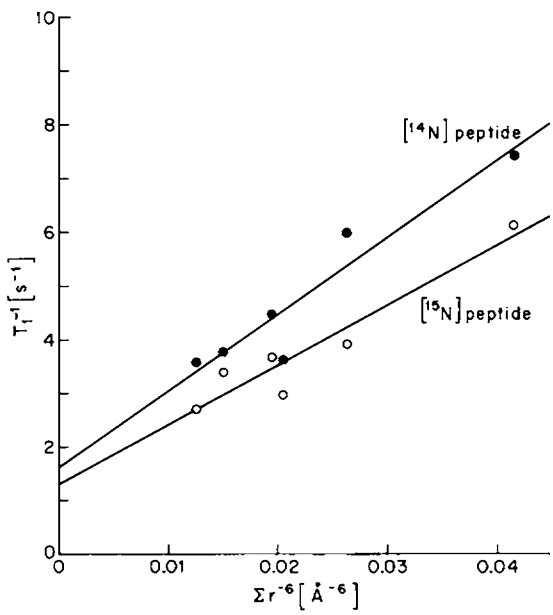

FIGURE 6 Linear test squares plot of proton T_1^{-1} versus distance parameter Σ for [^{14}N] and [^{15}N]alumichrome (220 MHz, 0.15 M solutions in d_6-DMSO, t = 44°C). The data are listed in Tables I and III.

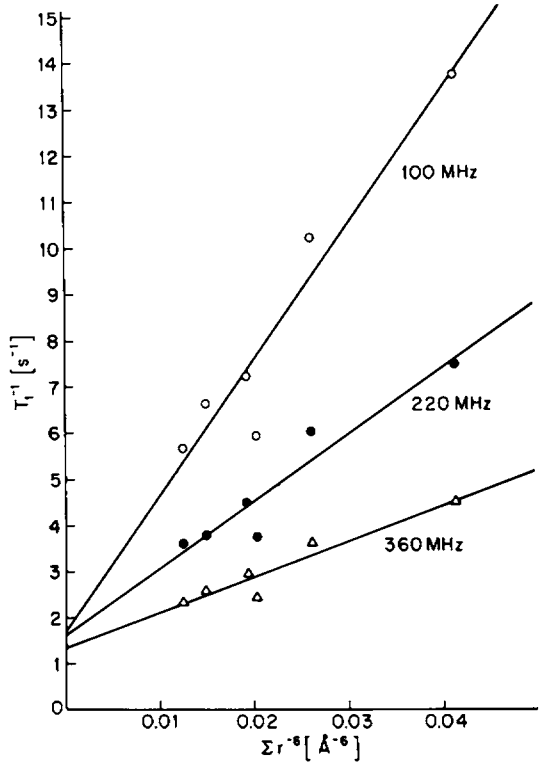

FIGURE 7 Field dependence of the alumichrome amide N*H* ^{1}H-NMR spin-lattice relaxation. Linear least squares plots of T_1^{-1} versus distance parameter Σ (0.15 M solution, t = 44°C). The data are listed in Tables II and III.

^{14}N peptide. Comparing the relaxation rates of alumichrome and [^{15}N]alumichrome (Table I) the predicted trend is seen to be satisfied by each of the amides. Fig. 6 shows the T_1^{-1} vs Σ plot for both peptides at 220 MHz, the linear least squares fits yielding T_1^{-1} = 143.7 Σ + 1.6 s^{-1}([^{14}N] peptide), and T_1^{-1} = 112.8 Σ + 1.3 s^{-1} ([^{15}N] peptide), both with correlation coefficients = 0.95. (Ideally, both lines should be parallel. The discrepancy most likely reflects experimental errors and the effect of fitting the magnetization recoveries with single exponentials.)

The field dependence of the amide proton spin-lattice relaxation shows that T_1's become longer at higher frequencies (Table II), while the slopes of the linear fits decrease (Fig. 7). This is what would be expected from the ω-dependence of $f(\omega, \tau_r)$ (Eq. 1), and it indicates that at high fields the Σ parameter plays a lesser role in determining the relaxation individuality of each amide. For alumichrome 10^{-8} s > $\tau_r \cong$ 4 × 10^{-10} s (8, 9), so that cross-relaxation plays no significant role at 100 MHz (3). Even at 360 MHz, where $(\omega\tau_r)^2$ = 0.84, we are fortuitously close to $(\omega\tau_r)^2$ = 5/4, the theoretical sign inversion point in the ω-dependence of cross-relaxation processes (see Eq. 7 in ref. 3). Hence, spin diffusion is truly negligible within the radiofrequency range we have investigated.

DISCUSSION

A most immediate consequence of this investigation is that the amides exhibit different spin-lattice thermal equilibria. This fact is relevant when integrated peak intensities are measured either in continuous wave or in correlation spectroscopy as the saturation characteristics of each proton are different (30).

As presented above, each linear fit provides two independent estimates of τ_r, one from the slope value ($^1H—^1H$ interaction) and the other from the intercept ($^1H—^{14}N$ or $^1H—^{15}N$ interaction). From the data on ^{14}N- and ^{15}N-alumichrome at 100, 220, and 360 MHz (Figs. 6 and 7), four linear fits were obtained and eight independent τ_r estimates derived (Table III), with an average $<\tau_r> = 3.58 \times 10^{-10}$ s. Confirming this estimate, $<\tau_r> = 3.97 \times 10^{-10}$ s was independently derived from the ratios of slopes and intercepts at any two fields. The overall internal consistency of these estimates is gratifying, especially if one considers that T_1 determinations on other heteronuclei have yielded $<\tau_r> \sim 4.1 \times 10^{-10}$ s (^{13}C) and $<\tau_r> \sim 3.8 \times 10^{-10}$ s (^{15}N) for alumichrome under identical solution conditions (8, 9).

The two ferrichrome crystallographic studies reported to date (15, 16) conclude fundamentally identical molecular shapes except in the configuration of the Orn^1 amide. In the case of ferrichrome A (15), this NH is pointing towards the pouch defined by the cyclohexapeptide backbone ring and the three ornithyl sidechains. The amide hydrogen atom is hence surrounded by a lipophilic enclosure and is considerably isolated from direct interaction with the molecular exterior. The picture is repeated in crystalline ferrichrysin (16), except that by rotating to a 19° larger ϕ angle, the Orn^1 NH points closer to the Orn^3 δ-*N*-hydroxy oxygen atom (N···O distance ~3.2 Å) suggesting the possibility of another H-bond. The authors (16) have speculated that this other H-bond would confer extra conformational stability to the molecule. Ferrichrome A and ferrichrysin both possess the same amino acid composition, the only difference being the hydroxamate acyl substituent, trans-β-methyl glutaconic acid in the first and acetic acid in the second (12). Except for resonances

TABLE III
LEAST SQUARES FIT $T_1^{-1} 2 A \cdot f(\omega, \tau_r) \Sigma r_{HH}^{-6} + B$
PARAMETERS AND DERIVED τ_r VALUES

Peptide	$\omega/2\pi$	Intercept data		Slope data	
		B	τ_r	$A \cdot f(\omega, \tau_r)$	τ_r
		s^{-1}	$s \times 10^{10}$	$Å^6 s^{-1}$	$s \times 10^{10}$
[^{14}N]alumichrome	100 MHz	1.69	2.79	291.59	4.20*
	220 MHz	1.61	3.07	143.69	2.19‡
	360 MHz	1.35	4.28	75.83	7.23
[^{15}N]alumichrome	220 MHz	1.29	3.51	112.84	1.35‡

The correlation coefficients for the least squares fits were >0.95 in all cases.
*Highest of two possible values.
‡Lowest of two possible values.

arising from the hydroxamate groups, the proton NMR spectra of alumichrome A and alumichrysin are essentially superimposable. The spectra do not reveal any difference in the extent of H bonding at the Orn^1 NH (18, 31). NMR investigations of a variety of alumichrome homologues, which differ in the residue occupancy of sites 2 and 3 Fig. 1) and/or in the nature of the coordinated ion [Al^{3+}, Ga^{3+}, or Co^{3+}, (17, 18, 24)] always detect the Orn^1 NH proton resonance at significantly higher fields, ca. 3.4 ppm closer to the tetramethylsilane (TMS) reference signal, than the strongly intramolecularly H-bonded Orn^2 NH resonance (Fig. 3). Furthermore, a variety of heteronuclear solvent perturbation experiments (19, 21, 24) and the positive slope of the temperature dependence of the amide proton resonance chemical shift, support a model where the Orn^1 NH does not interact with the solvent and it is not intramolecularly H bonded. When plotting the proton T_1^{-1} vs. the distance parameter Σ calculated from the ferrichrysin crystallographic coordinates (16), we consistently find larger deviations ($r \sim 0.7$) for the linear least squares fit than when using the ferrichrome A coordinates ($r > 0.9$). The discrepancy arises mainly from the exceedingly high values attributed to the Orn^1 NH Σ by the ferrichrysin coordinates because of positioning this proton closer to the ornithyl sidechain methylene protons ($\Sigma \gtrsim 0.0452$ Å^{-1}). It thus appears that for solution conditions, the crystallographic model of Zalkin et al. (15) best reflects the fine details of the molecular conformation of the Al^{3+}, Ga^{3+}, and Co^{3+} ferrichrome analogues examined to date. Given the similarity of the Ga^{3+}, Co^{3+}, and Fe^{3+} ionic radii [r_0 = 0.63 Å (32)], it is likely that the Orn^1 NH is not H-bonded in the ferric complex either, and that the hindrance of this amide to H-exchange with the solvent (14) is a consequence of its buried location only. The sixth power distance sensitivity of the NMR spin-lattice relaxation rate strongly supports this view and should, in other structurally rigid peptides, afford a definitive test of proposed conformational models.

The influence of ^1H—^{14}N dipolar interactions on the overall amide proton relaxation rates can have important consequences for the analysis of intramolecular ^1H—{^1H} nuclear Overhauser effect data. Norton and Allerhand (33) have shown that in the case of nonprotonated carbon atoms the ^{13}C—^{14}N dipolar interaction can govern the ^{13}C T_1 and hence significantly affect the magnitude of ^{13}C—{^1H} NOE's. As we are showing, the ^{14}N dipolar interaction also affects the amide ^1H T_1, so that the effective ^1H—{^1H} NOE between, e.g., NH and $C^\alpha H$, should be similarly reduced. Fig. 4 shows that although the ^{14}N—^1H relaxation is the same for all the amide protons, it represents a variable fraction of the overall rates. As exemplified by the Orn^3 amide, it can even be a major contributor to the observed NH proton relaxation rate. On the basis of the study of Bell and Saunders (34), ^1H—{^1H} NOE's are being increasingly exploited to derive dihedral angle and distance information in conformational investigations of peptide structures (ref. 35 and references therein). The present study calls for caution in interpreting such data when amide NH protons are observed in the NOE experiment. Since the relative contribution of the ^{14}N dipolar mechanism increases with frequency, at high fields the net amide ^1H—{^1H} NOE loses significance as a direct measure of molecular geometry. Yet even under such unfavorable conditions,

the r^{-6} dependence does manifest itself as a rate-determining factor in the buildup of the $^1H—\{^1H\}$ NOE (36), however small the latter may be, and quite independently of spin-diffusion. This points towards a need to re-evaluate interpretations of reported NH NOE's and to plan future experiments accordingly. Our findings also underline a fact that has not been emphasized enough: The assumptions involved in the Bell and Saunders approach (34) to derive internuclear distances are seldom proved valid and, as usually applied to polypeptide structural research, the method leaves much doubt regarding its soundness to quantitate conformational models.

The authors are indebted to Mr. W. Meier for his collaboration in preliminary aspects of this project and to Dr. E. S. de Llinás for computational assistance. Mr. R. Baumann, Dr. W. J. Horsley, and Dr. A. de Marco provided valuable help with the NMR spectroscopic work.

This project was sponsored by the Division of Biological and Environmental Research of the U.S. Department of Energy, the National Institutes of Health (grant NCI-1-RO-1-CA1428-1), and the Swiss National Science Foundation (grant 3.131.73).

Received for publication 8 May 1978 and in revised form 10 July 1978.

REFERENCES

1. KIMMICH, R., and F. NOAK. 1971. Nuclear magnetic relaxation in solutions of proteins and polypeptides. *Ber. Bunsenges. Phys. Chem.* **75**:269–272.
2. COATES, H. B., K. A. MCLAUCHLAN, I. D. CAMPBELL, and C. E. MCCOLL. 1973. Proton spin lattice relaxation time measurements at 90 MHz and 270 MHz. *Biochim. Biophys. Acta.* **310**:1–10.
3. SYKES, B. D., W. E. HULL, and G. H. SNYDER. 1978. Experimental evidence for the role of cross-relaxation in proton nuclear magnetic resonance spin lattice relaxation time measurements in proteins. *Biophys. J.* **21**:137–146.
4. SOLOMON, I. 1955. Relaxation processes in a system of two spins. *Phys. Rev.* **99**:559–565.
5. VOLD, R. L., J. S. WAUGH, M. P. KLEIN, and D. E. PHELPS. 1968. Measurement of spin relaxation in complex systems. *J. Chem. Phys.* **48**:3831–3832.
6. GUTOWSKY, H. S., and D. E. WOESSNER. 1956. Nuclear magnetic spin-lattice relaxation in liquids. *Phys. Rev.* **104**:843–844.
7. LYERLA, J. R., and G. C. LEVY. 1974. Carbon-13 nuclear spin relaxation. *Topics in Carbon-13 NMR Spectroscopy.* **1**:79–148.
8. LLINÁS, M., W. MEIER, and K. WÜTHRICH. 1977. A carbon-13 spin lattice relaxation study of alumichrome at 25.1 MHz and 90.5 MHz. *Biochim. Biophys. Acta.* **492**:1–11.
9. LLINÁS, M., and K. WÜTHRICH. 1978. A nitrogen-15 spin-lattice relaxation study of alumichrome. *Biochim. Biophys. Acta.* **532**:29–40.
10. KALK, A., and H. J. C. BERENDSEN. 1976. Proton magnetic relaxation and spin diffusion in proteins. *J. Magn. Resonance.* **24**:343–366.
11. BOTHNER-BY, A. A., and P. M. JOHNER. 1977. Spin-diffusion in macromolecules and its effect on nuclear Overhauser effects in proteins. *Proceedings XX C.S.I. and 7 I.C.A.S.*, Sborník Všcht v Praze, Prague, 355–372.
12. NEILANDS, J. B. 1973. Microbial iron transport compounds. *In* Inorganic Biochemistry. G. L. Eichhorn, editor, Elsevier Scientific Publishing Company, Amsterdam. 167–202.
13. EMERY, T. 1974. Biosynthesis and mechanism of action of hydroxamate-type siderochromes. *In* Microbial Iron Metabolism. J. B. Neilands, editor. Academic Press, Inc., New York. 107–124.
14. LLINÁS, M. 1973. Metal-polypeptide interactions: the conformational state of iron proteins. *Struct. Bonding.* **17**:139–151.
15. ZALKIN, A., J. D. FORRESTER, and D. H. TEMPLETON. 1966. Ferrichrome-A tetrahydrate. Determination of crystal and molecular structure. *J. Am. Chem. Soc.* **88**:1810–1814.
16. NORRESTAM, R., B. STENSLAND, and C. I. BRÄNDÉN. 1975. On the conformation of cyclic iron-containing hexapeptides: the crystal and molecular structure of ferrichrysin. *J. Mol. Biol.* **99**:501–506.

17. DEMARCO, A., M. LLINÁS, and K. WÜTRICH. 198. Analysis of the ^{1}H-NMR spectra of ferrichrome peptides. I. the non-amide protons. *Biopolymers.* **17**:617–636.
18. DEMARCO, A., M. LLINÁS, and K. WÜTHRICH. 1978. Analysis of the ^{1}H-NMR spectra of ferrichrome peptides. II. the amide resonance. *Biopolymers.* **17**:637–650.
19. LLINÁS, M., W. J. HORSLEY, and M. P. KLEIN. 1976. Nitrogen-15 nuclear magnetic resonance spectrum of alumichrome: detection by a double resonance Fourier transform technique. *J. Am. Chem. Soc.* **98**:7554–7558.
20. LLINÁS, M., D. M. WILSON, and J. B. NEILANDS. 1977. Peptide strain. Conformation dependence of the carbon-13 nuclear magnetic resonance chemical shifts in the ferrichromes. *J. Am. Chem. Soc.* **99**:3631–3637.
21. LLINÁS, M., D. M. WILSON, and M. P. KLEIN. 1977. Peptide hydrogen bonding. Conformation dependence of the carbonyl carbon-13 nuclear magnetic resonance chemical shifts in ferrichrome. A study by ^{13}C—{^{15}N} Fourier double resonance spectroscopy. *J. Am. Chem. Soc.* **99**:6846–6850.
22. URRY, D. W., and M. OHNISHI. 1970. Nuclear magnetic resonance and the conformation of cyclic polypeptide antibiotics. *In* Spectroscopic Approaches to Biomolecular Conformations. D. W. Urry, editor. American Medical Association, Ill. 263–300.
23. WYSSBROD, H. R., and W. A. GIBBONS. 1973. Conformation-function relationship in peptides and proteins. *Surv. Progr. Chem.* **6**:209–325.
24. LLINÁS, M., and M. P. KLEIN. 1975. Charge relay at the peptide bond. A proton magnetic resonance study of solvation effects on the amide electron density distribution. *J. Am. Chem. Soc.* **97**:4731–4737.
25. CUTNELL, J. D., J. A. GLASEL, and V. J. HRUBY. 1975. An investigation of contributions to carbon-13 spin-lattice relaxation in amino acids and peptide hormones. *Org. Magn. Resonance.* **7**:256–261.
26. PITNER, T. P., J. D. GLICKSON, R. ROWAN, J. DADOK, and A. A. BOTHNER-BY. 1975. Delineation of interactions between specific solvent and solute nuclei. A nuclear magnetic resonance solvent saturation study of Gramicidin S in methanol, dimethyl sulfoxide, and trifluorethanol. *J. Am. Chem. Soc.* **97**:5917–5918.
27. DESLAURIERS, R., G. C. LEVY, W. H. MCGREGOR, D. SARANTAKIS, and I. C. P. SMITH. 1977. The influence of glycyl residues on the flexibility of peptide hormones in solution. *Eur. J. Biochem.* **75**:343–346.
28. REDFIELD, A. G., and R. K. GUPTA. 1971. Pulsed-Fourier-transform nuclear magnetic resonance spectrometer. *Adv. Magn. Resonance* **5**:82–115.
29. ABRAGAM, A. 1961. The Principles of Nuclear Magnetism. Oxford University Press, London. 305–316.
30. LLINÁS, M. 1971. The solution conformation of the ferrichromes: statics and dynamics. Ph.D. dissertation. University of California, Berkeley.
31. LLINÁS, M., M. P. KLEIN, and J. B. NEILANDS. 1972. Solution conformation of the ferrichromes. III. A comparative proton magnetic resonance study of glycine- and serine-containing ferrichromes. *J. Mol. Biol.* **68**:265–284.
32. WEAST, R. C., editor. 1971. Crystal ionic radii of the elements. *In* Handbook of Chemistry and Physics. 52nd. edition. The Chemical Rubber Co., Ohio. F–171.
33. NORTON, R. S., and A. ALLERHAND. 1976. Effect of ^{13}C—^{14}N dipolar interactions on spin-lattice relaxation times and intensities of nonprotonated carbon atoms. *J. Am. Chem. Soc.* **98**:1007–1014.
34. BELL, R. A., and J. K. SAUNDERS. 1970. Correlation of the intramolecular nuclear Overhauser effect with internuclear distance. *Can J. Chem.* **48**:1114–1122.
35. BOTHNER-BY, A. A. 1979. Nuclear Overhauser effects in protons, and their use in the investigation of structures of biomolecules. *In* Magnetic Resonance Studies in Biology. R. G. Shulman, editor. Academic Press, Inc. New York. In press.
36. KUHLMANN, K. F., and D. M. GRANT. 1971. Carbon-13 relaxation and internal rotation in mesitylene and *o*-xylene. *J. Chem. Phys.* **55**:2998–3007.